Chem. Chem. Technol., 2023,
Vol. 17, No. 3, pp. 495–502

Chemistry

PECULIARITIES OF PHASE FORMATION IN SOL-GEL POWDERS OF THE $CaO–ZrO_2–Nb_2O_5–SiO_2$ SYSTEM

Iryna Lutsyuk[1, ✉], Yaryna Gavryshkevych[2], Yaroslav Vakhula[1]

https://doi.org/10.23939/chcht17.03.495

Abstract. The phase composition of xerogel powders of the $CaO–ZrO_2–Nb_2O_5–SiO_2$ system after heat treatment at 1273 K with different Nb_2O_5 content was established. The temperatures of the physical and chemical processes occurring during the powders heating were determined. It was found that the complete replacement of ZrO_2 by Nb_2O_5 resulted in the formation of niobium-containing phases with a change in the structure of the powders.

Keywords: phase formation, sol-gel technology, niobium and zirconium oxides, powder.

1. Introduction

The treatment of patients with chronic periodontitis is an urgent problem of modern endodontics due to their widespread prevalence, frequent complications, and the lack of stable results after traditional treatment.[1] According to numerous studies, the main principles of effective treatment of periodontitis destructive forms are a thorough instrumental and medicinal treatment of root canals with their further obturation with endohermetics. The purpose is to prevent microbial contamination and the influx of microbial factors into the surrounding tissues as well as to speed up the process of bone tissue restoration in the periapical area. The success of endodontic treatment is possible with the high-quality hermetic filling of the entire branched root canal system to create a reliable barrier between the tooth cavity and the periodontal tissues.[1]

Bioactive glass is of particular interest for use in endodontics, because its chemical composition (compounds of silicon, sodium, calcium, and phosphorus) is similar to the mineral composition of human bones and dentin.[2,3] Taking into account the significant biocompatibility, regenerative and antimicrobial properties of this material, and the fact that it has been used for more than forty years, its range of applications in dentistry is still not sufficient.

The bioactive glass paste contains at least one type of calcium silicate and at least one substantially anhydrous liquid. The term "substantially anhydrous" means completely anhydrous or containing water in so small amount that the paste does not undergo hydration and setting when stored in a hermetically sealed state. The amount of water in the carrier should not exceed 20 % of the paste weight.

Calcium silicate compounds, including mono-, di-, tricalcium silicate and their mixtures, can be used to make a paste. Ethyl alcohol, ethylene glycol, polyethylene glycol (PEG), glycerin liquid, glycerin, liquid organic acids, vegetable oil, animal oil, fish oil, and their mixtures are used as anhydrous liquid. The paste may contain water of hydration. The content of solid components in the paste is 60–90 wt. %, and the content of liquid ones is 10–40 wt. %. The amount of calcium silicate in the paste is on average from 30 to 70 wt. %. Other calcium compounds contained in the paste may include calcium oxide, hydroxide, carbonate, sulfate, calcium phosphate, and their mixtures. Phosphate compounds can be introduced into the paste mainly through phosphates of calcium, magnesium, zinc, ferrum, sodium, potassium, nickel, zirconium, phosphoric acid, and organometallic compounds. Calcium phosphates include di-, tri-, tetra-calcium phosphate, and their mixtures.

To improve the absorption of X-rays and, therefore, enhanced X-ray visualization, X-ray contrast materials containing barium sulfate, oxides of zirconium, bismuth, tantalum, and their mixtures are introduced into the paste composition. Zirconium oxide is the most commonly added X-ray contrast compound.[4]

Bioglass-based materials have pH > 7 and, accordingly, antibacterial activity, improved radiopacity, biocompatibility, low shrinkage, and chemical stability in biological environments.[5] The additional advantage of bioglass-based materials is that they promote the formation of hydroxyapatite, which ultimately improves the bond between the dentin and the root canal space-filling material during the curing process.[4,6–8]

However, traditional bioglass-based materials also have certain disadvantages, such as difficulties in working with them, high cytotoxicity in the freshly mixed state, a

[1] Lviv Polytechnic National University,
12, S. Bandery St., 79013 Lviv, Ukraine
[2] Danylo Halytsky Lviv National Medical University,
25b, Kutova St., 79014 Lviv, Ukraine
✉ *KhTS.dept@lpnu.ua*

long setting and curing time, which requires a corresponding moist environment. Moreover, one of the disadvantages of bioglass-based materials is that they are difficult to remove from the root canal if repeated endodontic treatment is required.[9]

Thus, the incorporation of new compounds into the composition of bioglass-based endohermetics makes it possible to improve the properties of these materials and eliminate their disadvantages.[10]

In this regard, the development of new bioglass-based materials for the obturation of root canals is a topical scientific research to improve the effectiveness of the treatment of pulp and periodontal diseases.

Taking into account the results of the chemical analysis of the commercial powders SURE-SEAL ROOT™ (SureDent, Korea) and BIO-C SEALER (Angelus, Brazil), the $CaO–ZrO_2–SiO_2$ system was taken as a basis. A large number of publications[11-15] on the effect of Nb_2O_5 on glass properties focused our attention on the partial replacement of ZrO_2 with Nb_2O_5 in existing compositions. Thus, the authors claim that the physical and optical properties of the sodium borosilicate glass are changed depending on the Nb_2O_5 content in its composition,[13] namely, with an increase in the Nb_2O_5 content, the glass transition temperature and glass density increase. The introduction of Nb_2O_5 into the composition of quartz glass leads to a shift of the characteristic thermal effects to the region of lower temperatures and an extension of the crystallization range.[14]

Scientists are interested in Nb_2O_5 not only in the cases of its use in the compositions of glass and crystalline oxide powders but also in the course of the sol-gel process with its participation. In this regard, the study of the processes that occur during the heat treatment of gels of the $CaO–ZrO_2–Nb_2O_5–SiO_2$ system is relevant.

The research aims to evaluate the effect of stepwise replacement of ZrO_2 by Nb_2O_5 on phase formation and to qualitatively determine the type of crystalline phases during heat treatment of sol-gel powders.

2. Experimental

The $CaO–ZrO_2–Nb_2O_5–SiO_2$ system, the powders of which were prepared by the sol-gel method, was chosen as the basis for the research. Crystal hydrates of calcium salts ($Ca(NO_3)_2·4H_2O$), zirconium ($ZrOCl_2·8H_2O$), niobium chloride $NbCl_5$, and ETS-40 were used as initial reagents. All substances were of chemically pure (CP) grade.

To obtain ETS-40 hydrolyzate, acidic sols were prepared, in which the concentrated nitric acid of the CP grade served as an acid catalyst in the amount of 0.6 wt. % relative to the total content of ethyl silicate and water, which ensures the solution pH of 1–2. To reduce the exothermic effect and the possibility of the most complete course of the hydrolysis process, the initial components were cooled to a temperature of 278–283 K. The detailed method of conducting hydrolysis is given in our previous work.[16]

Crystal hydrates of calcium and zirconium salts were dissolved in distilled water. Niobium chloride is insoluble in water, so to obtain a homogeneous solution a mixture of two organic solvents, namely acetone and isopropyl alcohol in a ratio of 1:1 (v/v) was used.

The resulting salt solutions were mixed in a certain stoichiometric ratio at room temperature and added dropwise to the ethyl silicate hydrolyzate under constant stirring on a magnetic stirrer for 0.5 h. The resulting solution was left for "maturation" until it completely turned into a gel, which was then dried at (373±5) K to obtain a xerogel. Heat treatment of xerogels was carried out at temperatures from 873 to 1273 K with isothermal exposure for 2 h.

Research on the processes of xerogels thermal decomposition was carried out using a Q-1500D derivatograph of the "Paulik-Paulik-Erdei" system connected to a personal computer. The samples were analyzed in the temperature range of 293–1273 K in the dynamic mode with a heating rate of 10 K/min in an air atmosphere. The reference substance was aluminum oxide. The weight of the samples was 100 mg.

X-ray phase analysis of the synthesized powders was carried out according to diffractograms obtained on a modernized DRON-3M diffractometer using CuKα radiation (λ = 1.54185 Å).

Electron microscopic studies were carried out using a SEM-16Y scanning electron microscope (Selmi). To increase the conductivity of the samples, a copper conductive film was applied to their surface by the thermovacuum sputtering method. The film thickness was no more than 50 nm. Microphotographs were processed using computer morphometry.

3. Results and Discussion

To choose the optimal conditions for the synthesis of powders of the $CaO–ZrO_2–Nb_2O_5–SiO_2$ system, a thermal analysis of xerogel samples of the nominal composition $20SiO_2·40CaO·(40-x)ZrO_2·xNb_2O_5$ was performed, where x = 1.0; 3.0; 5.0; 10.0; 20.0; 30.0; 40.0 (Fig. 1). The results of their complex thermal analysis are shown in the form of thermograms in Fig. 2, which include thermogravimetry (TG), differential thermogravimetry (DTG), and differential thermal analysis (DTA).

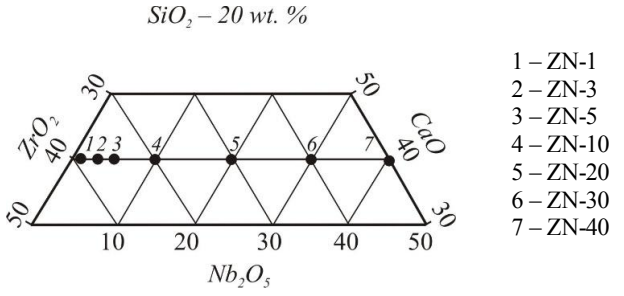

Fig. 1. Compositions of xerogel powders of the $CaO–ZrO_2–Nb_2O_5–SiO_2$ system

Thermal characteristics of samples ZN-1 and ZN-3 are similar. Thermolysis of the samples can be conditionally divided into five stages (Table 1).

Intensive mass loss of samples ZN-1 and ZN-3 occurs during the first three stages to the temperatures of 853 and 833 K, respectively. At the first stage of thermolysis in the temperature range of 343–473 K, significant mass loss is associated with the release of physically bound water, which is present in xerogels. In this case, mass loss is 23 wt. % for sample ZN-1 and 13 wt. % for ZN-3. This process is accompanied by rapid extrema on the DTG curves (t_{max} = 433 K) and the appearance of deep endothermic effects on the DTA curves (Fig. 2a,b) with maxima at temperatures of 453 K (ZN-1) and 443 K (ZN-3).

In the temperature range of 473–673(693) K, at the second stage of thermolysis, the release of crystallization water from calcium nitrate crystal hydrate and thermooxidative destruction of the organic component of the studied samples take place. They are accompanied by the mass loss of 17 wt. % and the appearance of inflections on the DTA curves with a maximum at a temperature of 633 K. At the same time, the DTA curves of both ZN-1 and ZN-3 samples show the transition of the endothermic effect to the exothermic one with a maximum at 583 K and 598 K, respectively.

At the third stage of thermolysis, in the temperature range of 693–853 K (sample ZN-1) and 673–833 K (sample ZN-3), the decomposition of calcium nitrate occurs and, accordingly, the release of gaseous decomposition products NO_2 and O_2. These processes correspond to the intense mass loss of the samples (19 and 17 wt. % for ZN-1 and ZN-3, respectively) on the TG curves, a clear extremum on the DTG curves with a maximum at 773–783 K, and the appearance of a deep endothermic effect with a maximum at 783–793 K on the DTA curves.

At temperatures above 823 K, at the fourth stage of thermolysis, the DTA curves deviate toward the region of exothermic effects with a maximum at 883 K (ZN-1) and 853 K (ZN-3). Since there is no change in the mass loss of the samples in the temperature ranges of 853–1003 K (ZN-1) and 833–993 K (ZN-3), these exoeffects can be obviously attributed to the ZrO_2 crystallization process.

With a further increase in temperature to 1273 K, at the fifth stage of thermolysis, the mass loss of the samples is insignificant (Δm = 3–5 wt. %), which probably corresponds to the final combustion of the carbonized residue of the xerogel samples.

Table 1. Thermogravimetric analysis of xerogels of the $CaO–ZrO_2–Nb_2O_5–SiO_2$ system

Sample	Stage of thermolysis	Temperature range, K	Mass loss, %
ZN-1	I	343–473	23
	II	473–693	17
	III	693–853	19
	IV	853–1003	0
	V	1003–1273	3
ZN-3	I	343–473	13
	II	473–673	17
	III	673–833	17
	IV	833–993	0
	V	993–1273	5
ZN-10	I	343–473	19
	II	473–713	18
	III	713–813	13
	IV	813–913	0
	V	913–1273	5
ZN-40	I	363–513	20
	II	513–733	13
	III	733–823	0
	IV	823–1193	12
	V	1193–1273	0

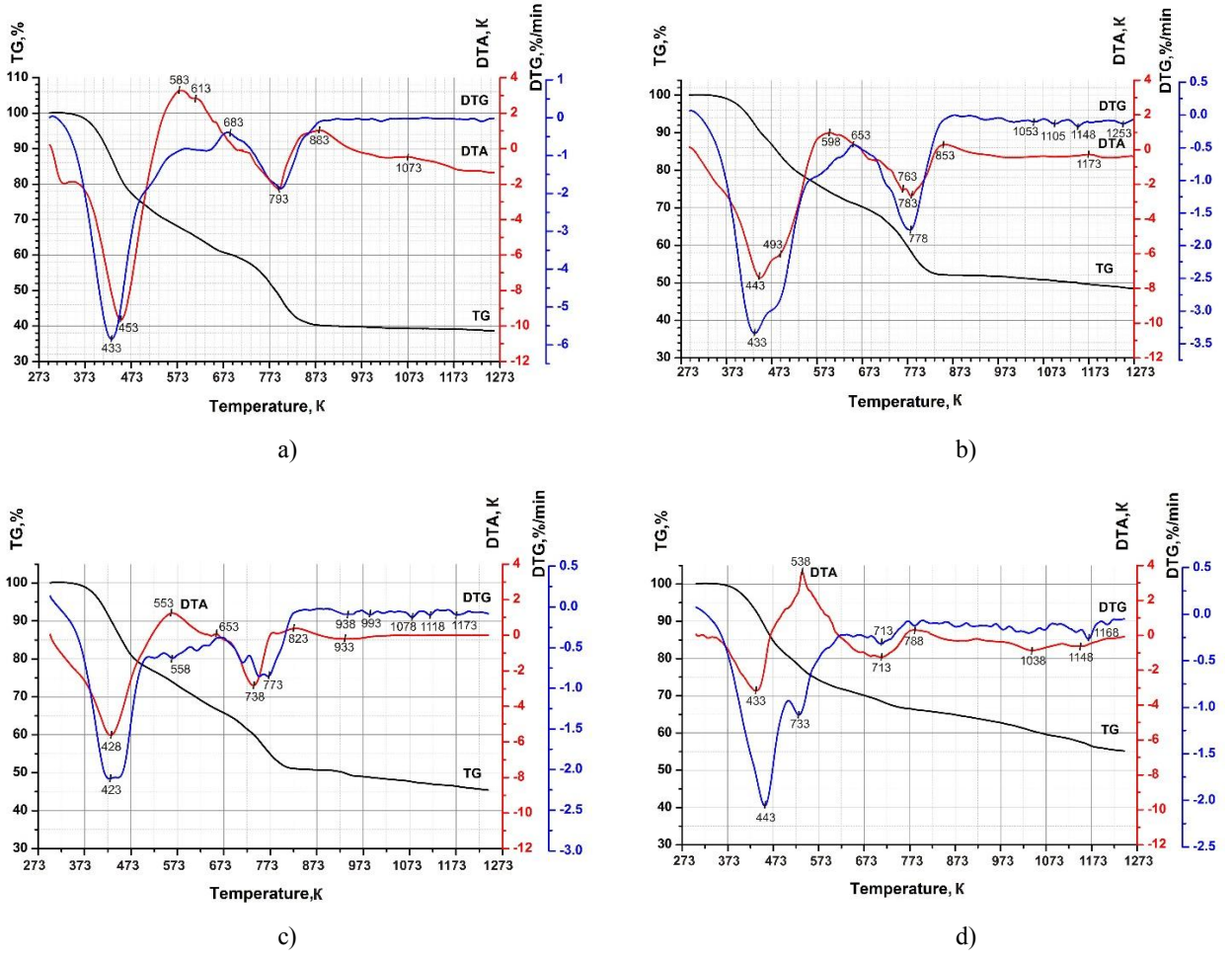

Fig. 2. Thermogravimetric analysis of xerogel powders of the $CaO–ZrO_2–Nb_2O_5–SiO_2$ system: ZN-1 (a); ZN-3 (b); ZN-10 (c) and ZN-40 (d)

Let us note that the DTA curves of the ZN-1 and ZN-3 samples show thermal effects corresponding to crystallization processes. The maximum of exothermic effect for the ZN-1 sample is observed at a temperature of 1073 K, and for the ZN-3 sample – at 1173 K. In our opinion, these data indicate the possible crystallization of $2CaO·SiO_2$.

The thermal processes which occur at various stages of the ZN-10 xerogel thermolysis (Fig. 2c) are similar to those in the ZN-1 and ZN-3 samples. However, it is worth noting that all processes are shifted towards lower temperatures, which is probably due to a somewhat smaller amount of organic components in the xerogel compositions.

The total mass loss of ZN-1, ZN-3, and ZN-10 samples is 62, 52, and 55 wt. %, respectively.

If ZrO_2 is completely replaced by Nb_2O_5 in the composition of the ZN-40 xerogel, a slightly lower mass loss is observed (Δm = 45 wt. %). As can be seen from the obtained TG curves (Fig. 2d), at the first stage of thermolysis in the temperature range of 363–513 K, there is a significant loss of sample mass (Δm = 20 wt. %), which is associated with the release of physically bound water. This process is accompanied by a deep extremum on the DTG curve (t_{max} = 443 K) and the appearance of an endothermic effect on the DTA curve with a maximum at a temperature of 433 K, which, in turn, gradually transfers into an exoeffect with a maximum at a temperature of 538 K. At the same time, at 513–733 K an intensive loss of the xerogel mass continues to take place, which is associated with the annealing of the organic component (Δm = 13 wt. %). The endothermic effect, which is manifested in the temperature range of 623–753 K with a maximum at 713 K, corresponds to the process of calcium nitrate decomposition and the release of volatile products. In the temperature range of 753–823 K with a maximum at 788 K, crystallization processes take place, which are accompanied by the appearance of a clear exothermic

effect on the DTA curve, without loss of sample mass. With a further increase in temperature to 1273 K, a monotonous mass loss is observed, which is 12 wt. %. At the same time, at the temperatures from 873 to 1223 K, the DTA curve has several inflections with maxima at the temperatures of 923, 1038, and 1148 K, which is probably related to the thermo-oxidative destruction of the organic component of the sample.

Using X-ray phase analysis, it was found that the ZN-1 sample heat-treated at a temperature below 873 K is an X-ray amorphous material. For the samples ZN-1 and ZN-3 the increase in processing temperature to 873 and 973 K results in the formation of reflections on the diffractograms belonging to ZrO_2 in the tetragonal modification, however, the nature of the diffractograms indicates its crytocrystalline structure (Fig. 3). During further annealing of the powders up to 1073 K, a slight narrowing of the diffraction peaks corresponding to ZrO_2 is observed. This is caused by the improvement of the material degree of crystallinity. At the same time, weak maxima corresponding to the crystalline phase of dicalcium silicate $2CaO·SiO_2$ appear on the diffractograms. The increase in processing temperature to 1173 K results in the intensity increase of all diffraction maxima. It should be noted that the peaks belonging to $2CaO·SiO_2$ are more intense for the ZN-1 sample compared to ZN-3.

A significant improvement in the structure of both ZrO_2 and $2CaO·SiO_2$ occurs only after samples annealing at 1273 K. An important point during the heat treatment of xerogels can be considered the crystallization of dicalcium silicate $2CaO·SiO_2$, the presence of which is desirable in dental compositions.

It is worth noting that the size of the formed crystallites, calculated according to Scherer's formula, is approximately 20 nm.

A comparative evaluation of the results of X-ray phase analysis of ZN-1 and ZN-3 samples showed that there is no significant difference between them, and the introduction of niobium oxide into the composition of sol-gel powders in the amount of up to 3 wt. % practically does not affect the phase and structure formation of the powders.

To study in detail the Nb_2O_5 effect on phase formation, the obtained gels were annealed at a temperature of 1273 K with isothermal holding for 2 h.

A detailed analysis of the diffractograms of all investigated powders makes allows us to assert the following: when ZrO_2 is replaced with niobium oxide Nb_2O_5 in the amount of 5 wt. % (sample ZN-5), the phase formation changes slightly (Fig. 4). Thus, the formation of $2CaO·SiO_2$ is not observed in the system; instead, the crystallization of dicalcium niobate $2CaO·Nb_2O_5$, silica takes place. ZrO_2 remains the main crystalline phase.

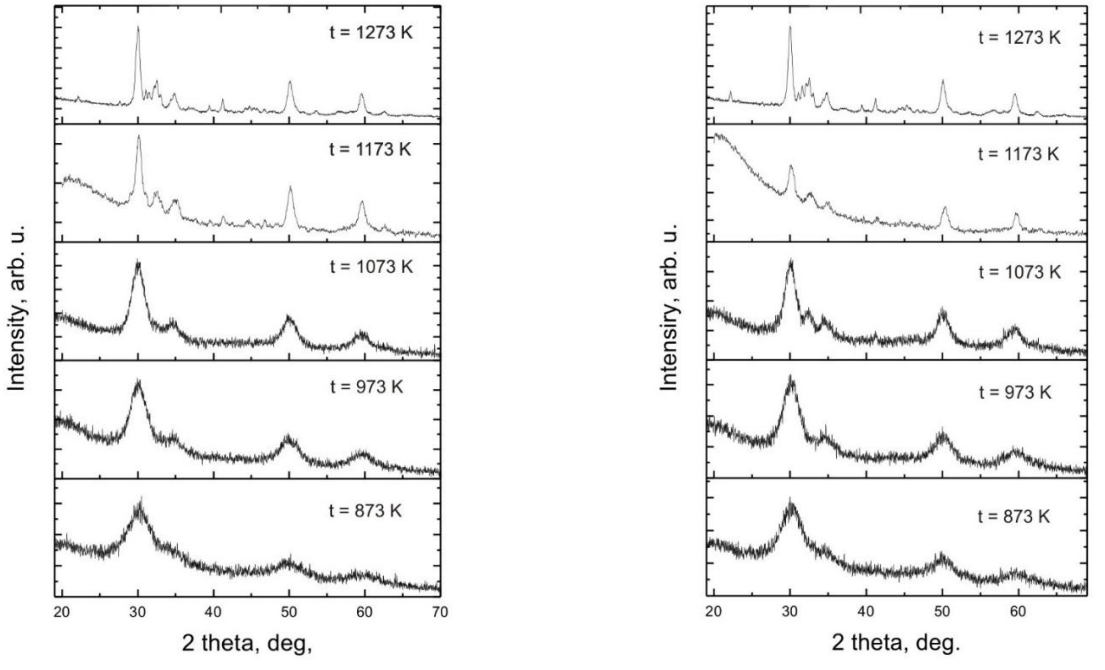

a) b)

Fig. 3. Change in the phase composition of powders of the SiO_2-CaO-ZrO_2-Nb_2O_5 system: ZN-1 (a) and ZN-3 (b) with temperature

Increasing the Nb_2O_5 content in the system to 10 wt. % does not qualitatively affect the change of crystalline phases (sample ZN-10). However, there is a strengthening of the lines belonging to $2CaO{\cdot}Nb_2O_5$. The lines corresponding to the ZrO_2 and SiO_2 content are weakened, which probably indicates the predominant role of dicalcium niobate in the powder structure. A similar pattern is observed for the Nb_2O_5 content of 20 wt. % (sample ZN-20).

The introduction of Nb_2O_5 in the amount of 30 wt. % (sample ZN-30) results in the formation of a multiphase system, containing apart from constantly present ZrO_2, a far less amount of niobium-containing phases $2CaO{\cdot}Nb_2O_5$ and $Ca_{6.5}Nb_{1.5}(Si_2O_7)_2O_4$. The crystallization of a new $CaZrO_3$ phase is observed as well.

In the case of the ZrO_2 complete replacement with Nb_2O_5 in the amount of 40 wt. % (sample ZN-40), a radical change in the phase composition of the powder takes place. The main crystalline phases are dicalcium niobate $2CaO{\cdot}Nb_2O_5$, monocalcium niobate $CaO{\cdot}Nb_2O_5$, and metacalcium silicate $CaSiO_3$.

The change in the phase composition of the powders of the $CaO–ZrO_2–Nb_2O_5–SiO_2$ system during heat treatment at 1273 K is shown in Table 2.

According to the SEM results, the microstructure of the ZN-1 sample obtained at a temperature of 1273 K is characterized by the presence of well-defined needle crystals of ZrO_2 badeleite (Fig. 5a). The size of the needles is in the range of 5 to 15 μm. The remaining crystalline phases of the sample are fixed in an undefined form.

Table 2. The composition of the crystalline phases of xerogels of the system $20SiO_2{\cdot}40CaO{\cdot}(40\text{-}x)ZrO_2{\cdot}xNb_2O_5$ after heat treatment (T = 1273 K, τ = 2 h)

ZN-1	ZN-3	ZN-5	ZN-10	ZN-20	ZN-30	ZN-40
ZrO_2 $2CaO{\cdot}SiO_2$	ZrO_2 $2CaO{\cdot}SiO_2$	ZrO_2 $2CaO{\cdot}Nb_2O_5$ SiO_2	ZrO_2 $2CaO{\cdot}Nb_2O_5$ SiO_2	ZrO_2 $4CaO{\cdot}Nb_2O_5$ SiO_2	ZrO_2 $Ca_{6,5}{\cdot}Nb_{1,5}{\cdot}(Si_2O_7)_2O_4$ $CaZrO_3$ $2CaO{\cdot}Nb_2O_5$	$2CaO{\cdot}Nb_2O_5$ $CaO{\cdot}Nb_2O_5$ $CaO{\cdot}SiO_2$

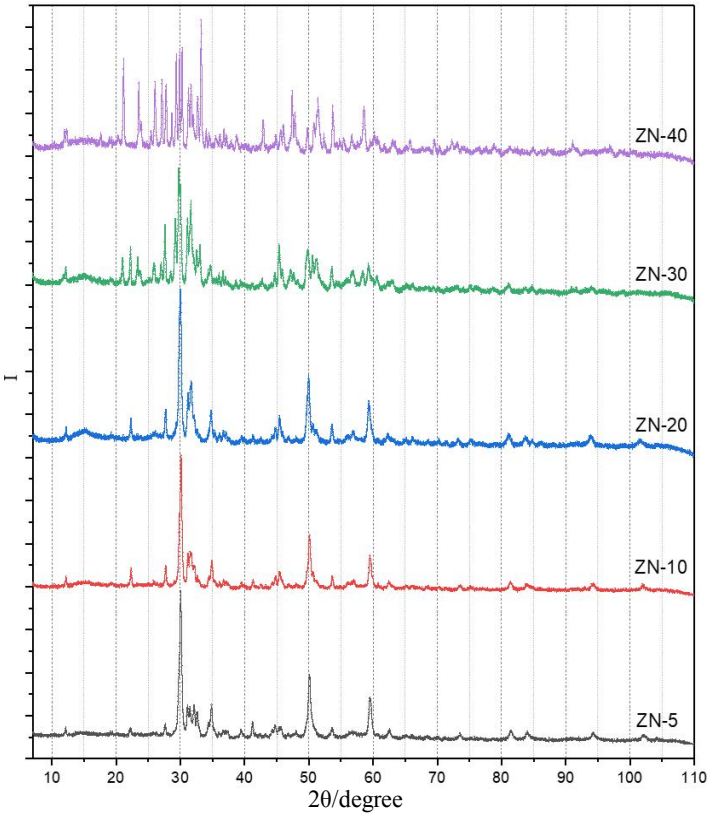

Fig. 4. Diffractograms of powders of the SiO_2-CaO-ZrO_2-Nb_2O_5 system. Heat treatment parameters (T = 1273 K, τ = 2 h)

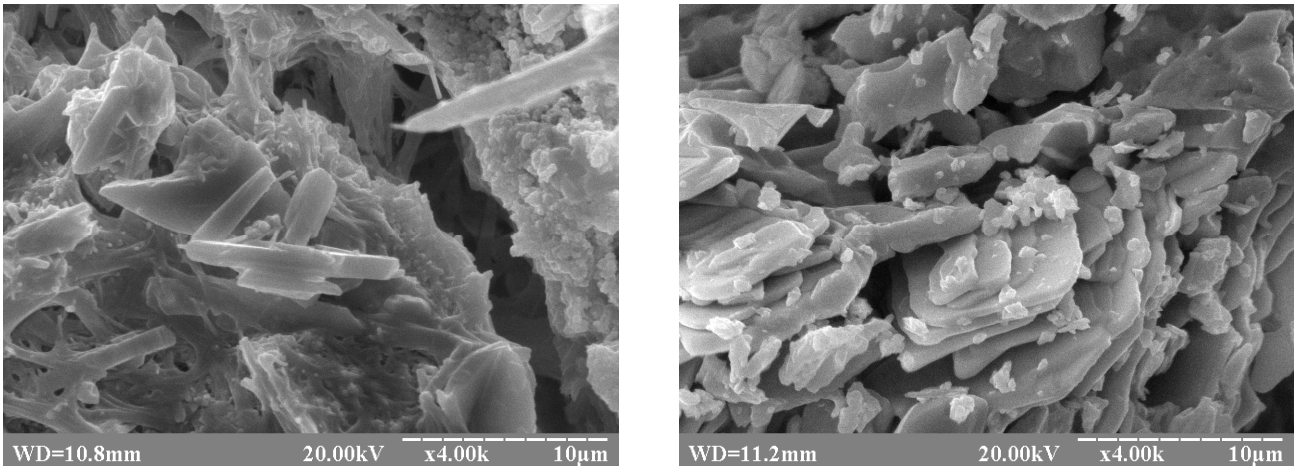

a) b)

Fig. 5. Electron micrographs of ZN-1 (a) and ZN-40 (b) structures

The ZN-40 sample (Fig. 5b) is characterized by a structure consisting of separate aggregate blocks formed by parallel-oriented layers. Such a layered structure has the appearance of scales without a clearly defined shape and is characteristic of dicalcium niobate. The spaces between individual layers are filled with smaller crystals of 1 to 2 μm in size.

4. Conclusions

Taking into account the positive effect of niobium oxide on the properties of glass and medical oxide powders of the $CaO–ZrO_2–Nb_2O_5–SiO_2$ system, they have been modified with Nb_2O_5 to improve their performance.

The crystallization temperature of powders obtained from xerogels by sol-gel technology was found to begin at 873 K with the formation of ZrO_2 as the main phase. An increase in the processing temperature contributes to the formation of an additional crystalline phase – calcium silicate. X-ray phase analysis showed that the introduction of niobium oxide into the composition of gels in the amount of 5 wt. % changes the qualitative phase composition of the powders, in particular, the formation of niobium-containing phases, namely dicalcium niobate $2CaO·Nb_2O_5$. When ZrO_2 is completely replaced with Nb_2O_5, mono- and dicalcium niobate as well as wollastonite $CaO·SiO_2$ are crystallized.

Differential thermal analysis of the powders showed that the increase in the Nb_2O_5 amount decreases the intensity of ZrO_2 crystallization, and its crystallization temperature shifts to lower values.

Additional studies of powders with different amounts of Nb_2O_5 will make it possible to recommend individual compositions for effective use in dentistry.

References

[1] Rotstein, I.; Salehrabi, R.; Forrest, J. L. Endodontic Treatment Outcome: Survey of Oral Health Care Professionals. *J. Endod.* **2006**, *32*, 399-403. https://doi.org/10.1016/j.joen.2005.10.056
[2] Baino, F.; Novajra, G.; Miguez-Pacheco, V.; Boccaccini, A. R.; Vitale-Brovarone, C. Bioactive Glasses: Special Applications Outside the Skeletal System. *J. Non Cryst. Solids* **2016**, *432*, 15-30. https://doi.org/10.1016/j.jnoncrysol.2015.02.015
[3] Dubok, V. A. Bioceramics – Yesterday, Today, Tomorrow. *Powder Metall. Met. Ceram.* **2000**, *39*, 381-394. https://doi.org/10.1023/A:1026617607548
[4] Yang, Q.; Lu, D. Premixed Biological Hydraulic Cement Paste Composition and Using the Same. US 2008/O299.093 A1, 04 December 2008.
[5] El-Saady Badawy, R.; Mohamed, D.A. Evaluation of New Bioceramic Endodontic Sealers: An *in vitro* Study. *Dent Med Probl* **2022**, *59*, 85-92. https://doi.org/10.17219/dmp/133954
[6] Chellapandian, K.; Reddy, T. V. K.; Venkatesh, V.; Annapurani, A. Bioceramic Root Canal Sealers: A Review. *Int. J. Health Sci.* **2022**, *6*, 5693-5706. https://doi.org/10.53730/ijhs.v6nS3.7214
[7] Kohli, M.R.; Karabucak, B. Bioceramic Usage in Endodontics. *Bioceramics* 2019. https://www.aae.org/specialty/communique/bioceramic-usage-in-endodontics
[8] Chybowski, EA; Glickman, GN; Patel, Y.; Fleury, A.; Solomon, E.; He, J. Clinical Outcome of Non-Surgical Root Canal Treatment Using a Single-cone Technique with Endosequence Bioceramic Sealer: A Retrospective Analysis. *J Endod.* **2018**, *44*, 941-945. https://doi.org/10.1016/j.joen.2018.02.019
[9] Candeiro, G. T.; Correia, F. C.; Duarte, M. A.; Ribeiro-Siqueira, D. C.; Gavini, G. Evaluation of Radiopacity, pH, Release of Calcium Ions, and Flow of a Bioceramic Root Canal Sealer. *J Endod.* **2012**, *38*, 842-845. https://doi.org/10.1016/j.joen.2012.02.029
[10] Hench, L. L. Genetic Design of Bioactive Glass. *J. Eur. Ceram. Soc.* **2009**, *29*, 1257-1265. https://doi.org/10.1016/j.jeurceramsoc.2008.08.002
[11] Bertolini, M. J.; Palma-Dibb, R. G.; Zaghete, M. A.; Gimenes, R. Evaluation of Glass Ionomer Cements Properties Obtained from

Niobium Silicate Glasses Prepared by Chemical Process. *J Non Cryst Solids* **2005**, *351*, 466-471. https://doi.org/10.1016/j.jnoncrysol.2005.01.040
[12] Fliberg, S. R.; Silberberg, Y.; Oliver, M. K.; Andrejco, M. J.; Saifi, M. A.; Smith P. W. Ultrafast All□Optical Switching in a Dual□Core Fiber Nonlinear Coupler. *Appl. Phys. Lett*. **1987**, *51*, 1135-1137. https://doi.org/10.1063/1.98762
[13] Cardinal, T.; Fargin, E.; Le Flem, G. Non Linear Optical Properties of Some Niobium (V) Oxide Glasses. *Eur. J. Solids State Inorg. Chem*. **1996**, *33*, 597-605.
[14] Samuneve, B.; Kralchev, St.; Dimitrof, V. Structure and Optical Properties of Niobium Silicate Glasses. *J. Non Cryst. Solids* **1991**, *129*, 54-63. https://doi.org/10.1016/0022-3093(91)90080-P
[15] Graca, M. P. F.; Valente, M. A.; Ferreira da Silva, M. G. Electrical Properties of Lithium Niobium Silicate Glasses. *J. Non Cryst. Solids* **2003**, *325*, 267-274. https://doi.org/10.1016/S0022-3093(03)00314-4
[16] Lutsyuk, I.; Vakhula, Ya.; Tupis, I.; Iliuchok, I. Catalytic Action of Nitric Acid on The Hydrolysis of ETS-40 Ethyl Silicate. *Chem. Chem. Technol*. **2021**, *15*, 475-478. https://doi.org/10.23939/chcht15.04.475

Received: February 14, 2023 / Revised: March 09, 2023 / Accepted: March 25, 2023

ОСОБЛИВОСТІ ФАЗОУТВОРЕННЯ В ЗОЛЬ-ГЕЛЬ ПОРОШКАХ СИСТЕМИ $CaO–ZrO_2–Nb_2O_5–SiO_2$

Анотація. *Встановлено фазовий склад порошків ксерогелів системи $CaO–ZrO_2–Nb_2O_5–SiO_2$ після термооброблення за 1273 K із різним вмістом Nb_2O_5. Визначено температури фізико-хімічних процесів, що відбуваються під час нагрівання порошків. Встановлено, що за повної заміни ZrO_2 на Nb_2O_5 має місце утворення ніобійвмісних фаз зі зміною структури порошків.*

Ключові слова: *фазоутворення, золь-гель технологія, ніобію та цирконію оксиди, порошки.*